



**NO<sub>x</sub> emission estimates during the 2014 Youth Olympic Games in Nanjing**

J. Ding et al.

# NO<sub>x</sub> emission estimates during the 2014 Youth Olympic Games in Nanjing

J. Ding<sup>1,2</sup>, R. J. van der A<sup>1</sup>, B. Mijling<sup>1</sup>, P. F. Levelt<sup>1,2</sup>, and N. Hao<sup>3</sup>

<sup>1</sup>Royal Netherlands Meteorological Institute (KNMI), De Bilt, the Netherlands

<sup>2</sup>Delft University of Technology, Delft, the Netherlands

<sup>3</sup>German Aerospace Center (DLR), Oberpfaffenhofen, Germany

Received: 12 February 2015 – Accepted: 23 February 2015 – Published: 4 March 2015

Correspondence to: J. Ding (jieding.ding@knmi.nl)

Published by Copernicus Publications on behalf of the European Geosciences Union.

Title Page

Abstract

Introduction

Conclusions

References

Tables

Figures



Back

Close

Full Screen / Esc

Printer-friendly Version

Interactive Discussion



## Abstract

The Nanjing Government has taken temporary environmental regulations to guarantee good air quality during the Youth Olympic Games (YOG) in 2014. We study the effect of those regulations by applying the emission estimate algorithm DECSO (Daily Emission estimates Constrained by Satellite Observations) to measurements of the Ozone Monitoring Instrument (OMI). We improved DECSO by updating the chemical transport model CHIMERE from v2006 to v2013 and by adding an Observation minus Forecast (OmF) criterion to filter outlying satellite retrievals due to high aerosol concentrations. The comparison of model results with both ground and satellite observations indicates that CHIMERE v2013 is better performing than CHIMERE v2006. After filtering the satellite observations with high aerosol loads that were leading to large OmF values, unrealistic jumps in the emission estimates are removed. Despite the cloudy conditions during the YOG we could still see a decrease of tropospheric NO<sub>2</sub> column concentrations of about 32 % in the OMI observations as compared to the average NO<sub>2</sub> concentrations from 2005 to 2012. The results of the improved DECSO algorithm for NO<sub>x</sub> emissions show a reduction of at least 25 % during the YOG period. This indicates that air quality regulations taken by the local government were successful. The algorithm is also able to detect an emission reduction of 10 % during the Chinese Spring Festival. This study demonstrates the capacity of the DECSO algorithm to capture the change of NO<sub>x</sub> emissions on a monthly scale. We also show that the observed concentrations and the derived emissions show different patterns that provide complimentary information. For example, the Nanjing smog episode in December 2013 led to a strong increase in NO<sub>2</sub> concentrations without an increase in NO<sub>x</sub> emissions. Furthermore, DECSO gives us important information of the non-trivial seasonal relation between NO<sub>x</sub> emissions and NO<sub>2</sub> concentrations on a local scale.

## NO<sub>x</sub> emission estimates during the 2014 Youth Olympic Games in Nanjing

J. Ding et al.

Title Page

Abstract

Introduction

Conclusions

References

Tables

Figures



Back

Close

Full Screen / Esc

Printer-friendly Version

Interactive Discussion



## 1 Introduction

Reducing air pollution is one of the biggest environmental challenges currently in China. Nearly 75 % of urban areas are regularly polluted in a way that is considered unsuitable for their inhabitants in 2004 (Shao et al., 2006). In mega cities and their immediate vicinities, air pollutants exceed the Chinese Grade-II standard ( $80 \mu\text{g m}^{-3}$  for daily  $\text{NO}_2$ ) on 10–30 % of the days (Chan and Yao, 2008). Air pollution is directly related to the economic growth in China and its accompanying increase of energy consumption. In the last two decades, air pollutants persistently increased in China. For instance, satellite measurements showed that  $\text{NO}_2$  concentrations increased about  $20 \%$  year<sup>-1</sup> from 1996 to 2005 (van der A et al., 2006). By combining satellite observations with air quality models, Itahashi et al. (2014) showed that the strong increase of  $\text{NO}_2$  concentrations over East China is caused by a doubling of  $\text{NO}_x$  ( $\text{NO}_x = \text{NO} + \text{NO}_2$ ) emissions during 2000 to 2010. Zhang et al. (2007) found that  $\text{NO}_x$  emissions increased with 70 % between 1995 and 2006 and Lamsal et al. (2011) found that anthropogenic  $\text{NO}_x$  emissions increased with 18.8 % during the period 2006 to 2009.

Nanjing, the capital of Jiangsu Province, is a highly urbanized and industrialized city located in East China, in the northwest part of the Yangtze River Delta (YRD). By 2012, the area of Nanjing had a population of 8.2 million (Nanjing statistical Bureau, 2013). The YRD is one of the largest economic and most polluted regions in China. Tu et al. (2007) found that the largest fraction of air pollution by  $\text{NO}_x$  and  $\text{SO}_2$  can be attributed to local sources in Nanjing. Li et al. (2011) concluded that air pollutant concentrations and visibility demanded urgent air pollution regulations in the YRD region. From 16 to 29 August 2014, the Youth Olympic Games (YOG) was held in Nanjing. To guarantee good air quality during the Games, the city government carried out temporary strict environmental regulations with 35 directives from May to August. Other cities in the YRD cooperated with Nanjing to ensure good air quality during the Games. The periods with the main regulations are shown in Table 1.

### **NO<sub>x</sub> emission estimates during the 2014 Youth Olympic Games in Nanjing**

J. Ding et al.

Title Page

Abstract

Introduction

Conclusions

References

Tables

Figures



Back

Close

Full Screen / Esc

Printer-friendly Version

Interactive Discussion







satellite observations of OMI, taking advantage of its high spatial resolution needed to resolve the changes in the Nanjing area. With this improved algorithm we will compare the NO<sub>x</sub> emissions during the YOG with NO<sub>x</sub> emissions of the previous year in Yangtze Delta River.

## 2 Methods

### 2.1 Emission estimates

For the emission estimates of NO<sub>x</sub> over China we use the DECSO algorithm (Mijling and van der A, 2012). It uses a CTM to simulate the NO<sub>2</sub> concentrations and daily satellite observations of NO<sub>2</sub> column concentrations to constrain NO<sub>x</sub> emissions. The algorithm is based on an extended Kalman filter to get new emission estimates by optimizing NO<sub>2</sub> column concentrations of model and satellite observations. The inclusion of sensitivities of NO<sub>2</sub> column concentrations on the NO<sub>x</sub> emissions in other locations is an essential part of DECSO. A terrain-following trajectory analysis is used in this calculation to describe the transport of NO<sub>2</sub> over the model domain for a time interval between two overpasses of the satellite instrument. This approach results in a fast algorithm suitable for daily estimates of NO<sub>x</sub> emissions. A detailed description of DECSO v1 can be found in Mijling and van der A (2012).

The CTM used in DECSO is CHIMERE (Schmidt, 2001; Bessagnet et al., 2004; Menut et al., 2013). CHIMERE is implemented on a 0.25° × 0.25° spatial grid over East Asia from 18 to 50° N and 102 to 132° E. It contains 8 atmospheric layers up to 500 hPa. The meteorological input for CHIMERE is the operational meteorological forecast of the European Centre for Medium-Range Weather Forecasts (ECMWF) with a horizontal resolution of approximately 25 km × 25 km. The Multi-resolution Emission Inventory for China (MEIC) (He, 2012) for 2010 gridded to a resolution of 0.25° × 0.25°, is used for the initial emissions in DECSO. Outside China, where no MEIC emissions are defined, the emission inventory of INTEX-B (Q. Zhang et al., 2009) is used. As the emission sector

## NO<sub>x</sub> emission estimates during the 2014 Youth Olympic Games in Nanjing

J. Ding et al.

Title Page

Abstract

Introduction

Conclusions

References

Tables

Figures



Back

Close

Full Screen / Esc

Printer-friendly Version

Interactive Discussion



definition used in MEIC and INTEX-B does not match the 11 activity sectors according to the SNAP (Selected Nomenclature for Air Pollution) 97, which are internally used in the CHIMERE model, we redistribute the emissions over the sectors according to Table 2.

To compare CHIMERE simulations with satellite observations, we extend the modelled vertical profiles from 500 hPa to the tropopause by adding a climatological partial column. The simulated NO<sub>2</sub> column concentrations on the model grid are redistributed to the satellite footprints. To enable direct comparison between simulated and observed tropospheric vertical column, the averaging kernel from the satellite retrieval is then applied to the modelled vertical profile.

In this study, we used an updated version of DECSO, which is referred to as DECSO v3. Especially the calculation speed has been improved in this update. Furthermore, the emission injection height has been made sector-dependent and the forward trajectory calculation is changed to a backward calculation. In DECSO v3, the error  $E_{\text{obs}}$  of a satellite observation is recalculated according to:

$$E_{\text{obs}} = f \cdot E_{\text{sat}} + (1 - f) \cdot (0.5 \cdot E_{\text{sat}}), \quad \text{with } f = e^{\left(-\frac{c_{\text{sat}}}{2}\right)} \quad (1)$$

where  $E_{\text{sat}}$  is the observation error from the retrieval method and  $c_{\text{sat}}$  is the retrieved NO<sub>2</sub> column of the satellite observation. The modified errors give more weight to satellite observations with high values during the assimilation by reducing their relative error while maintaining the dominating absolute error for low values (typically around  $0.5 \times 10^{15}$  molecules cm<sup>-2</sup>).

## 2.2 Satellite observations

In this study, satellite observations from the Dutch-Finnish Ozone Monitoring Instrument (OMI) on NASA's (National Aeronautics and Space Administration) Aura satellite (Levelt et al., 2006) are used in DECSO. The satellite was launched on 15 July 2004 into a sun-synchronous polar orbit at 705 km altitude. OMI is a nadir-viewing spec-

Title Page

Abstract

Introduction

Conclusions

References

Tables

Figures

◀

▶

◀

▶

Back

Close

Full Screen / Esc

Printer-friendly Version

Interactive Discussion









### 3 Improvements of DECSO

#### 3.1 Model improvement

The performance of the CTM is important for the DECSO results. CHIMERE v2006 is an outdated model version which has been used in DECSO algorithm versions up to v3a. To improve the emission estimation results, we updated the CTM to CHIMERE v2013 (DECSO v3b).

The new model adds biogenic emissions of six species: isoprene,  $\alpha$ -ioporene,  $\alpha$ -pinene,  $\beta$ -pinene, limonene, ocimene and NO. These biogenic emissions are calculated by the model preprocessor using the MEGAN model and land use data (Menut et al., 2013). The added biogenic emissions can affect the emissions estimated for rural areas as biogenic NO emissions in rural areas cannot be negligible in summertime. Compared to the old version of CHIMERE, the new model version includes a more advanced scheme for secondary organic aerosol chemistry. In addition, the chemical reaction rates are updated and a new transport scheme is used in the new CHIMERE model. For CHIMERE v2013 we use the same input data except for the land use data. We use land use data from the GlobCover Land Cover (GCLC version 2.3) database, which is updated for the year 2009, while the land use database included in CHIMERE v2006 is the Global Land Cover Facility (GLFC) giving the land use of 1994. As China is a fast developing country, the land use may have large differences in 15 years due to urbanization. Thus, the updated land use database will positively affect the model simulations over China.

To assess the effect of the new CTM, we run DECSO v3a and DECSO v3b for the period January 2013 to August 2014. Figure 1 shows the comparison of the average diurnal cycle of surface NO<sub>2</sub> concentrations from the two CHIMERE models with in-situ observations in Nanjing averaged for January to August 2014. We select the 0.25° × 0.25° model grid cell that contains the in-situ measurement location. According to GCLC database, 70 % of the grid cell is urban area. We see that the surface NO<sub>2</sub> concentration of CHIMERE v2013 during nighttime is closer to the observations than

## NO<sub>x</sub> emission estimates during the 2014 Youth Olympic Games in Nanjing

J. Ding et al.

Title Page

Abstract

Introduction

Conclusions

References

Tables

Figures



Back

Close

Full Screen / Esc

Printer-friendly Version

Interactive Discussion





















covers on average a larger area than a single grid cell. To achieve emission estimates in a smaller area, either satellite observations with a higher spatial resolution are required, or longer time periods should be considered.

The quality of our emission estimates is highly related to the quality of the model and the satellite observations. We improved the DECSO algorithm by using a new version of the CTM: CHIMERE v2013 instead of CHIMERE v2006. The comparison of OmF between two models showed that CHIMERE v2013 has a better performance in summer-time. Good quality of satellite observations is also essential for emission estimates. The DOMINO retrieval algorithm does not properly account for the effects of high aerosol concentrations, which are common in China, on the retrieved NO<sub>2</sub> columns. In case of high aerosol concentrations, the difference of the model simulations and the retrievals is very large, which leads to wrong updates of NO<sub>x</sub> emission in DECSO. To improve the satellite observations we have set an OmF criterion to filter out erroneous observations and to avoid unrealistic NO<sub>x</sub> emission updates. We set the limitation to the range -5 to 10 × 10<sup>15</sup> molecules cm<sup>-2</sup> for the OmF. With this filter criterion, the unrealistic updates of NO<sub>x</sub> emissions are mostly prevented. We will further analysis the impact of high aerosol concentrations on the retrieved NO<sub>2</sub> columns in future research.

Furthermore, we observed an opposite seasonal cycle of NO<sub>x</sub> emissions compared to the NO<sub>2</sub> concentrations observed by OMI satellite. The seasonal cycle of NO<sub>x</sub> emissions is not the same for the whole China domain since the different climate in the North and the South of China leads to a different variability of energy consumption during the year. In Nanjing, as in most parts of Southern China, people use air conditioning in summer and do not use heating systems in winter. This leads to larger electricity consumptions of power plants in summer causing higher NO<sub>x</sub> emissions. Tu et al. (2007) studied the air pollutants in Nanjing and also found high NO<sub>2</sub> concentrations in winter but concluded that the high NO<sub>2</sub> concentrations were caused by high NO<sub>x</sub> emissions in winter, while our emission estimates show the opposite. Wang et al. (2007) analyzed the seasonality of NO<sub>x</sub> emissions based on GOME satellite observations for the regions north and south of Yangtze River, defined as north and south China. Their re-

## NO<sub>x</sub> emission estimates during the 2014 Youth Olympic Games in Nanjing

J. Ding et al.

Title Page

Abstract

Introduction

Conclusions

References

Tables

Figures



Back

Close

Full Screen / Esc

Printer-friendly Version

Interactive Discussion



sults of south China showed the same seasonal cycle of NO<sub>2</sub> columns but a very weak seasonality of NO<sub>x</sub> emissions and they also concluded that the NO<sub>x</sub> lifetime mainly determines the NO<sub>2</sub> columns.

In conclusion, in the emission estimates we not only found a reversed seasonal cycle peaking in summertime, but also indications for reduced emissions during the Spring Festival, the Asian Youth Games in 2013 and the YOG 2014. Based on our emission estimates the air quality regulation during the YOG 2014 reduced the NO<sub>x</sub> emissions with at least 25 % . This, together with favorable meteorological conditions, was responsible for the decrease of 32 % in NO<sub>2</sub> column concentrations observed from space. For the case of the YOG, our results can help the local government to identify the impact of their air quality regulations on reducing NO<sub>x</sub> emissions.

*Acknowledgements.* The research was part of the GlobEmission Project funded and supported by the European Space Agency. We acknowledge Tsinghua University for providing the MEIC inventory and the ESA GlobCover 2009 Project for the land use dataset. The MODIS images used in this study were acquired as part of the NASA's Earth-Sun System Division and archived and distributed by the MODIS Adaptive Processing System (MODAPS). The OMI is part of the NASA Earth Observing System (EOS) Aura satellite payload. The OMI project is managed by the Netherlands Space Office (NSO) and the Royal Netherlands Meteorological Institute (KNMI).

## References

- Bessagnet, B., Hodzic, A., Vautard, R., Beekmann, M., Cheinet, S., Honoré, C., Liousse, C., and Rouil, L.: Aerosol modeling with CHIMERE – preliminary evaluation at the continental scale, *Atmos. Environ.*, 38, 2803–2817, doi:10.1016/j.atmosenv.2004.02.034, 2004.
- Blond, N., Boersma, K. F., Eskes, H. J., van der A, R. J., Van Roozendael, M., De Smedt, I., Bergametti, G., and Vautard, R.: Intercomparison of SCIAMACHY nitrogen dioxide observations, in situ measurements and air quality modeling results over Western Europe, *J. Geophys. Res.*, 112, 1–20, doi:10.1029/2006JD007277, 2007.

## NO<sub>x</sub> emission estimates during the 2014 Youth Olympic Games in Nanjing

J. Ding et al.

Title Page

Abstract

Introduction

Conclusions

References

Tables

Figures



Back

Close

Full Screen / Esc

Printer-friendly Version

Interactive Discussion





**NO<sub>x</sub> emission estimates during the 2014 Youth Olympic Games in Nanjing**

J. Ding et al.

Title Page

Abstract

Introduction

Conclusions

References

Tables

Figures



Back

Close

Full Screen / Esc

Printer-friendly Version

Interactive Discussion



Lamsal, L. N., Martin, R. V., Padmanabhan, A., van Donkelaar, A., Zhang, Q., Sioris, C. E., Chance, K., Kurosu, T. P., and Newchurch, M. J.: Application of satellite observations for timely updates to global anthropogenic NO<sub>x</sub> emission inventories, *Geophys. Res. Lett.*, **38**, L05810, doi:10.1029/2010GL046476, 2011.

Levelt, P. F., van den Oord, G. H. J., Dobber, M. R., Malkki, A., Stammes, P., Lundell, J. O. V., and Saari, H.: The ozone monitoring instrument, *IEEE T. Geosci. Remote*, **44**, 1093–1101, doi:10.1109/TGRS.2006.872333, 2006.

Li, L., Chen, C. H., Fu, J. S., Huang, C., Streets, D. G., Huang, H. Y., Zhang, G. F., Wang, Y. J., Jang, C. J., Wang, H. L., Chen, Y. R., and Fu, J. M.: Air quality and emissions in the Yangtze River Delta, China, *Atmos. Chem. Phys.*, **11**, 1621–1639, doi:10.5194/acp-11-1621-2011, 2011.

Liu, H., Wang, X., Zhang, J., He, K., Wu, Y., and Xu, J.: Emission controls and changes in air quality in Guangzhou during the Asian Games, *Atmos. Environ.*, **76**, 81–93, doi:10.1016/j.atmosenv.2012.08.004, 2013.

Martin, R. V., Jacob, D. J., Kurosu, T. P., Chance, K., Palmer, P. I., and Evans, M. J.: Global inventory of nitrogen oxide emissions constrained by space-based observations of NO<sub>2</sub> columns, *J. Geophys. Res.*, **108**, 4537, doi:10.1029/2003JD003453, 2003.

Menut, L., Bessagnet, B., Khvorostyanov, D., Beekmann, M., Blond, N., Colette, A., Coll, I., Curci, G., Foret, G., Hodzic, A., Mailler, S., Meleux, F., Monge, J.-L., Pison, I., Siour, G., Turquety, S., Valari, M., Vautard, R., and Vivanco, M. G.: CHIMERE 2013: a model for regional atmospheric composition modelling, *Geosci. Model Dev.*, **6**, 981–1028, doi:10.5194/gmd-6-981-2013, 2013.

Mijling, B., van der A, R. J., Boersma, K. F., Van Roozendaal, M., De Smedt, I., and Kelder, H. M.: Reductions of NO<sub>2</sub> detected from space during the 2008 Beijing Olympic Games, *Geophys. Res. Lett.*, **36**, L13801, doi:10.1029/2009GL038943, 2009.

Mijling, B. and van der A, R. J.: Using daily satellite observations to estimate emissions of short-lived air pollutants on a mesoscopic scale, *J. Geophys. Res.-Atmos.*, **117**, D17302, doi:10.1029/2012JD017817, 2012.

Miyazaki, K., Eskes, H. J., Sudo, K., Takigawa, M., van Weele, M., and Boersma, K. F.: Simultaneous assimilation of satellite NO<sub>2</sub>, O<sub>3</sub>, CO, and HNO<sub>3</sub> data for the analysis of tropospheric chemical composition and emissions, *Atmos. Chem. Phys.*, **12**, 9545–9579, doi:10.5194/acp-12-9545-2012, 2012.

**NO<sub>x</sub> emission estimates during the 2014 Youth Olympic Games in Nanjing**

J. Ding et al.

[Title Page](#)[Abstract](#)[Introduction](#)[Conclusions](#)[References](#)[Tables](#)[Figures](#)[⏪](#)[⏩](#)[◀](#)[▶](#)[Back](#)[Close](#)[Full Screen / Esc](#)[Printer-friendly Version](#)[Interactive Discussion](#)

Schmidt, H.: A comparison of simulated and observed ozone mixing ratios for the summer of 1998 in Western Europe, *Atmos. Environ.*, 35, 6277–6297, doi:10.1016/S1352-2310(01)00451-4, 2001.

Shao, M., Tang, X., Zhang, Y., and Li, W.: City clusters in China: air and surface water pollution, *Front. Ecol. Environ.*, 4, 353–361, doi:10.1890/1540-9295(2006)004[0353:CCICAA]2.0.CO;2, 2006.

Stavrakou, T., Müller, J.-F., Boersma, K. F., De Smedt, I., and van der A, R. J.: Assessing the distribution and growth rates of NO<sub>x</sub> emission sources by inverting a 10-year record of NO<sub>2</sub> satellite columns, *Geophys. Res. Lett.*, 35, L10801, doi:10.1029/2008GL033521, 2008.

Streets, D. G., Canty, T., Carmichael, G. R., de Foy, B., Dickerson, R. R., Duncan, B. N., Edwards, D. P., Haynes, J. A., Henze, D. K., Houyoux, M. R., Jacob, D. J., Krotkov, N. A., Lamsal, L. N., Liu, Y., Lu, Z., Martin, R. V., Pfister, G. G., Pinder, R. W., Salawitch, R. J., and Wecht, K. J.: Emissions estimation from satellite retrievals: a review of current capability, *Atmos. Environ.*, 77, 1011–1042, doi:10.1016/j.atmosenv.2013.05.051, 2013.

Tu, J., Xia, Z.-G., Wang, H., and Li, W.: Temporal variations in surface ozone and its precursors and meteorological effects at an urban site in China, *Atmos. Res.*, 85, 310–337, doi:10.1016/j.atmosres.2007.02.003, 2007.

Van der A, R. J., Peters, D. H. M. U., Eskes, H., Boersma, K. F., Van Roozendael, M., De Smedt, I., and Kelder, H. M.: Detection of the trend and seasonal variation in tropospheric NO<sub>2</sub> over China, *J. Geophys. Res.*, 111, D12317, doi:10.1029/2005JD006594, 2006.

Wang, S., Zhao, M., Xing, J., Wu, Y., Zhou, Y., Lei, Y., He, K., Fu, L., and Hao, J.: Quantifying the air pollutants emission reduction during the 2008 olympic games in Beijing, *Environ. Sci. Technol.*, 44, 2490–2496, 2010.

Wang, Y., McElroy, M. B., Martin, R. V., Streets, D. G., Zhang, Q., and Fu, T. M.: Seasonal variability of NO<sub>x</sub> emissions over east China constrained by satellite observations: implications for combustion and microbial sources, *J. Geophys. Res.-Atmos.*, 112, 1–19, doi:10.1029/2006JD007538, 2007.

Wang, Y., Hao, J., McElroy, M. B., Munger, J. W., Ma, H., Chen, D., and Nielsen, C. P.: Ozone air quality during the 2008 Beijing Olympics: effectiveness of emission restrictions, *Atmos. Chem. Phys.*, 9, 5237–5251, doi:10.5194/acp-9-5237-2009, 2009.

Witte, J. C., Schoeberl, M. R., Douglass, A. R., Gleason, J. F., Krotkov, N. A., Gille, J. C., Pickering, K. E., and Livesey, N.: Satellite observations of changes in air quality dur-

ing the 2008 Beijing Olympics and Paralympics, Geophys. Res. Lett., 36, L17803, doi:10.1029/2009GL039236, 2009.

Zhang, H., Sun, Z., Zhen, Y., Zhang, X., and Yu, B.: Impact of temperature change on urban electric power load in Nanjing, Trans. Atmos. Sci., 32, 536–542, 2009.

5 Zhang, Q., Streets, D. G., He, K., Wang, Y., Richter, A., Burrows, J. P., Uno, I., Jang, C. J., Chen, D., Yao, Z., and Lei, Y.: NO<sub>x</sub> emission trends for China, 1995–2004: the view from the ground and the view from space, J. Geophys. Res., 112, D22306, doi:10.1029/2007JD008684, 2007.

10 Zhang, Q., Streets, D. G., Carmichael, G. R., He, K. B., Huo, H., Kannari, A., Klimont, Z., Park, I. S., Reddy, S., Fu, J. S., Chen, D., Duan, L., Lei, Y., Wang, L. T., and Yao, Z. L.: Asian emissions in 2006 for the NASA INTEX-B mission, Atmos. Chem. Phys., 9, 5131–5153, doi:10.5194/acp-9-5131-2009, 2009.

15 Zhao, C. and Wang, Y.: Assimilated inversion of NO<sub>x</sub> emissions over east Asia using OMI NO<sub>2</sub> column measurements, Geophys. Res. Lett., 36, L06805, doi:10.1029/2008GL037123, 2009.

**NO<sub>x</sub> emission estimates during the 2014 Youth Olympic Games in Nanjing**

J. Ding et al.

Title Page

Abstract

Introduction

Conclusions

References

Tables

Figures



Back

Close

Full Screen / Esc

Printer-friendly Version

Interactive Discussion







## NO<sub>x</sub> emission estimates during the 2014 Youth Olympic Games in Nanjing

J. Ding et al.

Title Page

Abstract

Introduction

Conclusions

References

Tables

Figures

◀

▶

◀

▶

Back

Close

Full Screen / Esc

Printer-friendly Version

Interactive Discussion



**Table 2.** Redistribution of MEIC sectors over SNAP 97 sectors.

SNAP 97 sectors	MEIC sectors	Power	Industry	Transport	Residential	Agriculture
Combustion in energy and transformation industries		1	–	–	–	–
Non-industrial combustion plants		–	–	–	1	–
Combustion in manufacturing industry		–	0.3	–	–	–
Production process		–	0.3	–	–	–
Extraction and distribution of fossil fuels and geothermal energy		–	0.4	–	–	–
Solvent and other product use		–	–	–	–	–
Road transport		–	–	1	–	–
Other mobile sources and machinery		–	–	–	–	–
Waste treatment and disposal		–	–	–	–	–
Agriculture		–	–	–	–	1
Other source and sinks		–	–	–	–	–



## NO<sub>x</sub> emission estimates during the 2014 Youth Olympic Games in Nanjing

J. Ding et al.

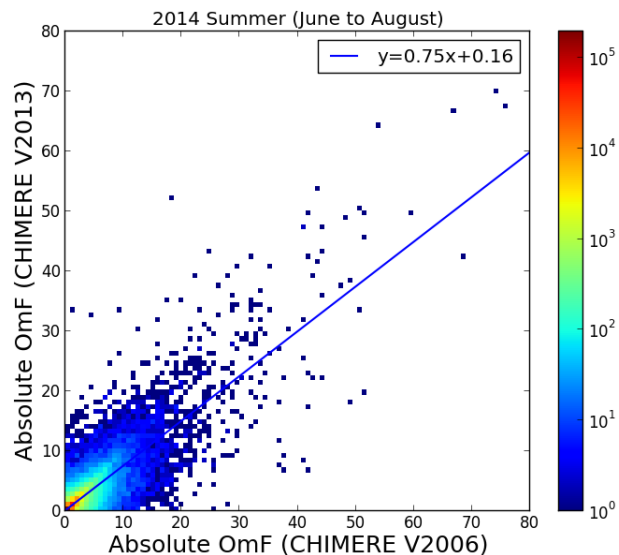


**Figure 2.** The comparison of the absolute OmF ( $10^{15}$  molecules  $\text{cm}^{-2}$ ) of CHIMERE v2006 and CHIMERE v2013.

[Title Page](#)[Abstract](#)[Introduction](#)[Conclusions](#)[References](#)[Tables](#)[Figures](#)[◀](#)[▶](#)[◀](#)[▶](#)[Back](#)[Close](#)[Full Screen / Esc](#)[Printer-friendly Version](#)[Interactive Discussion](#)

**NO<sub>x</sub> emission estimates during the 2014 Youth Olympic Games in Nanjing**

J. Ding et al.

Title Page

Abstract

Introduction

Conclusions

References

Tables

Figures



Back

Close

Full Screen / Esc

Printer-friendly Version

Interactive Discussion

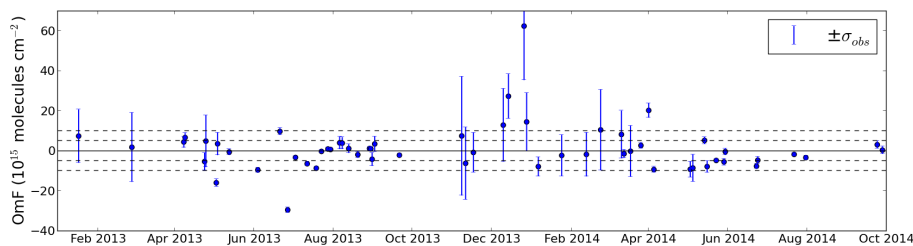


**Figure 3.** The time series of the OmF from January 2013 to September 2014. The error bar is the root mean square error of observations ( $\sigma_{\text{obs}}$ ).









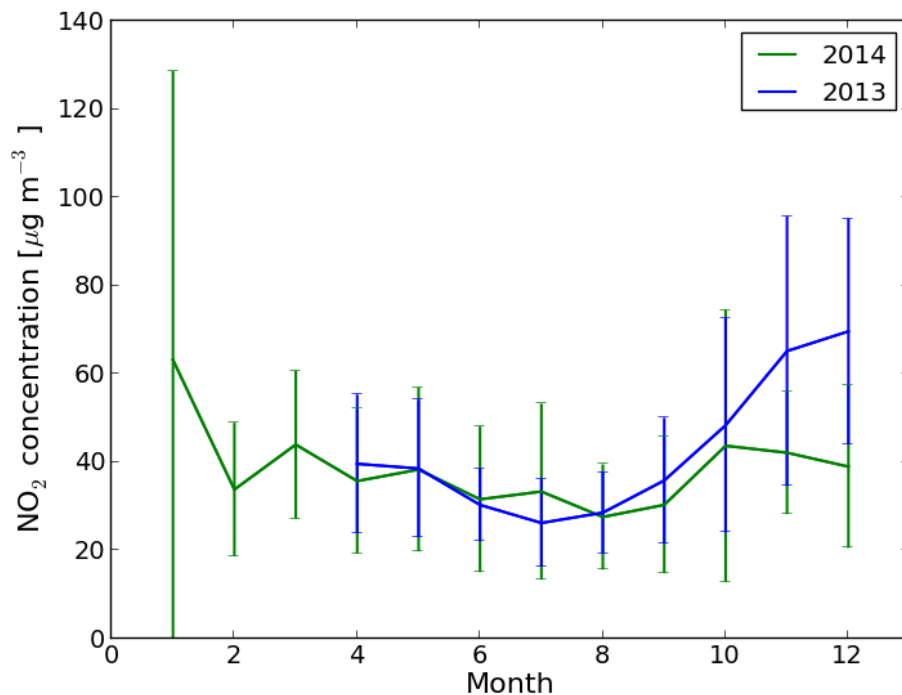


**Figure 7.** The monthly averaged in-situ NO<sub>2</sub> concentration at 13 local time in Nanjing for 2013 and 2014. The error bar is the SD (natural variability) of the observations for each month (derived from the daily data on [www.aqicn.org](http://www.aqicn.org)).

**NO<sub>x</sub> emission estimates during the 2014 Youth Olympic Games in Nanjing**

J. Ding et al.

Title Page

Abstract Introduction

Conclusions References

Tables Figures

◀ ▶

◀ ▶

Back Close

Full Screen / Esc

Printer-friendly Version

Interactive Discussion



## NO<sub>x</sub> emission estimates during the 2014 Youth Olympic Games in Nanjing

J. Ding et al.

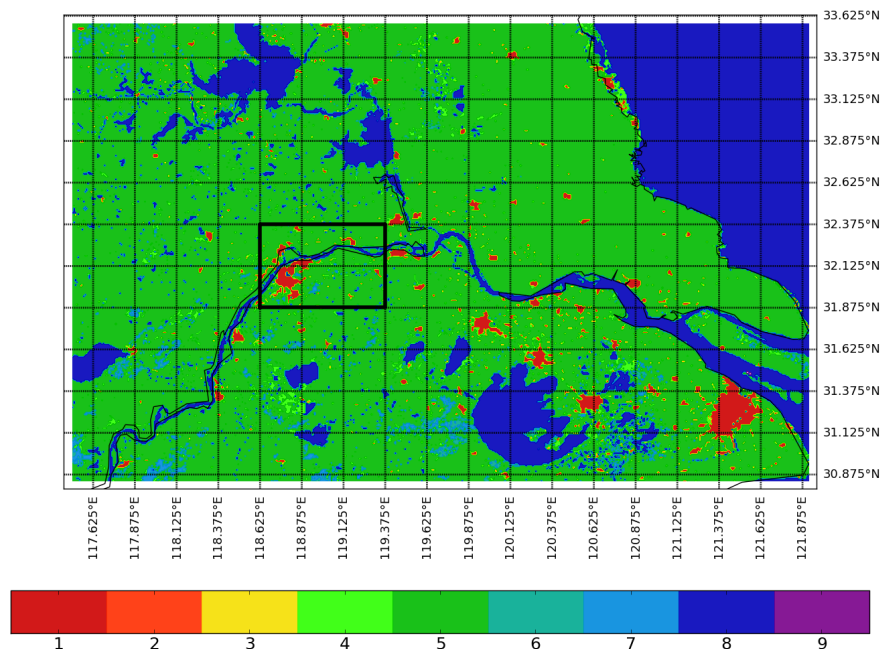


**Figure 8.** Land use over the Jiangsu Province as used in CHIMERE v2013. The 9 categories are: 1. Urban, 2. Barren land, 3. Grassland, 4. Agricultural land, 5. Shrubs, 6. Needleleaf forest, 7. Broadleaf forest, 8. Ocean, 9. Inland water. The solid rectangle indicates the 6 grid cells that cover the Nanjing area.

[Title Page](#)[Abstract](#)[Introduction](#)[Conclusions](#)[References](#)[Tables](#)[Figures](#)[Back](#)[Close](#)[Full Screen / Esc](#)[Printer-friendly Version](#)[Interactive Discussion](#)

## NO<sub>x</sub> emission estimates during the 2014 Youth Olympic Games in Nanjing

J. Ding et al.

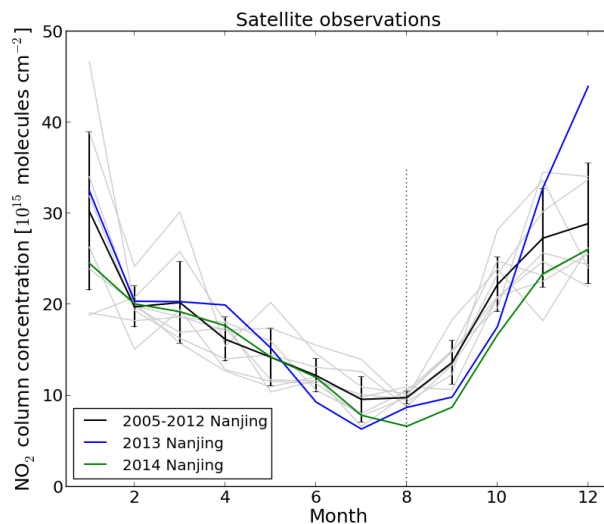


**Figure 9.** The monthly averages of OMI satellite observations of tropospheric NO<sub>2</sub> concentrations. The solid lines are the measurements over the Nanjing area. The grey lines are the monthly averages for each year from 2005 to 2012 to indicate the annual variability. The black lines show the average value for the years from 2005 to 2012. The errorbars are the SD of monthly NO<sub>2</sub> observations from 2005 to 2012.

[Title Page](#)[Abstract](#)[Introduction](#)[Conclusions](#)[References](#)[Tables](#)[Figures](#)[◀](#)[▶](#)[◀](#)[▶](#)[Back](#)[Close](#)[Full Screen / Esc](#)[Printer-friendly Version](#)[Interactive Discussion](#)

## NO<sub>x</sub> emission estimates during the 2014 Youth Olympic Games in Nanjing

J. Ding et al.

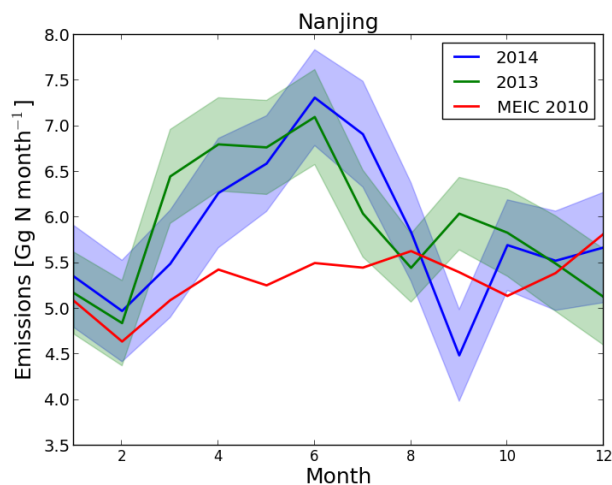


**Figure 10.** The monthly NO<sub>x</sub> emission estimates by DECSO in Nanjing for 2013 (green line) and 2014 (blue line) and the monthly NO<sub>x</sub> emission of the MEIC inventory of 2010 (red line). The shade areas show the error of the mean NO<sub>x</sub> emission estimates from DECSO.

[Title Page](#)[Abstract](#)[Introduction](#)[Conclusions](#)[References](#)[Tables](#)[Figures](#)[◀](#)[▶](#)[◀](#)[▶](#)[Back](#)[Close](#)[Full Screen / Esc](#)[Printer-friendly Version](#)[Interactive Discussion](#)